Available online at www.sciencedirect.com
ScienceDirect
Acta Materialia 59 (2011) 5320–5331
Acta MATERIALIA
www.elsevier.com/locate/actamat

Orientation relationships of copper crystals on c-plane sapphire

Stefano Curiotto [a,*], Harry Chien [b], Hila Meltzman [c], Paul Wynblatt [b], Gregory S. Rohrer [b], Wayne D. Kaplan [c], Dominique Chatain [a]

[a] CNRS, Aix-Marseille University, CINAM-UPR3118, Campus de Luminy, F-13288 Marseille, France
[b] Department of Materials Science and Engineering, Carnegie Mellon University, Pittsburgh, PA 15213, USA
[c] Department of Materials Engineering, Technion – Israel Institute of Technology, Haifa 32000, Israel

Received 7 February 2011; received in revised form 19 April 2011; accepted 1 May 2011
Available online 3 June 2011

Abstract

Copper particles have been grown on sapphire (0 0 0 1) substrates by dewetting a copper film either in the solid or the liquid state. After equilibration the particles adopt different orientation relationships (ORs). Solid state dewetting produces a single OR: Cu(1 1 1)[1 $\bar{1}$ 0]||Al_2O_3(0 0 0 1)[1 0 $\bar{1}$ 0]. In contrast, dewetting in the liquid state (followed by solid state equilibration) produces four additional ORs, Cu(1 1 1) [1 $\bar{1}$ 0]||Al_2O_3(0 0 0 1)[2 $\bar{1}$ $\bar{1}$ 0], Cu(1 1 0)[1 $\bar{1}$ 0]||Al_2O_3(0 0 0 1)[2 $\bar{1}$ $\bar{1}$ 0], Cu(3 1 1)[0 1 $\bar{1}$]||Al_2O_3(0 0 0 1)[2 $\bar{1}$ $\bar{1}$ 0] and Cu(2 1 0)[0 0 1]||Al_2O_3(0 0 0 1) [2 $\bar{1}$ $\bar{1}$ 0], which have been found to have a similar interfacial energy. All of the ORs observed in this study are consistent with the Fecht and Gleiter lock-in model, from which one would expect that densely packed directions in the interface plane of the metal crystals will tend to align with relatively dense directions in the substrate surface. The 30° change in alignment direction on the c-sapphire side of the interface, from Al_2O_3 [1 0 $\bar{1}$ 0] for solid state dewetted samples to Al_2O_3 [2 $\bar{1}$ $\bar{1}$ 0] for samples dewetted in the liquid state, appears to be related to a reconstruction of the copper–c-sapphire interface that occurs at a temperature between those at which the two types of samples are processed.

Keywords: Alumina (α-Al_2O_3); Copper; Electron backscattered diffraction; Orientation relationship; Interface energy

1. Introduction

The interfacial properties of metal–oxide systems have been of considerable interest over the past several years in applications such as integrated circuits and metal–ceramic joining. The stability of the bond between the metal and the oxide depends in large part on the metal–oxide interfacial energy, which is in turn related to the orientation relationships (ORs) at the interface, as well as the microscopic interfacial structure and chemistry.

In this work copper on sapphire (α-Al_2O_3) was selected as a model system for the study of metal–oxide interfaces, and for the investigation of the ORs of metals on oxide substrates. Much of the previous work on the copper–sapphire system has focused on the OR of solid copper films deposited (usually from the vapor phase) on (0 0 0 1) oriented (i.e. c-sapphire) substrates [1–6]. The most frequent OR identified in these studies was Cu(1 1 1) [1 $\bar{1}$ 0]||Al_2O_3(0 0 0 1) [1 0 $\bar{1}$ 0], which we shall refer to in this paper as OR1, although Bialas and Knoll [4], Scheu et al. [5] and Oh et al. [6] also observed another OR: Cu(1 1 1) [1 $\bar{1}$ 0]||Al_2O_3(0 0 0 1) [2 $\bar{1}$ $\bar{1}$ 0], which we shall refer to as OR2.

In addition to thin film studies of ORs, Fecht and Gleiter [7] investigated the ORs that develop between particles of gold or copper deposited on the surfaces of a number of ionic substrates of various orientations. This approach was an extension of the seminal work of Herrmann et al. [8], in which copper particles were deposited on copper single crystal substrates in order to study the relative energies of grain boundaries in copper. The concept behind these experiments is that a particle deposited in an initially random orientation on the substrate would tend to rotate into an OR that represents a low energy cusp in

* Corresponding author.
E-mail address: curiotto@cinam.univ-mrs.fr (S. Curiotto).

1359-6454/$36.00 © 2011 Acta Materialia Inc. Published by Elsevier Ltd. All rights reserved.
doi:10.1016/j.actamat.2011.05.008

the orientation dependence of interfacial energy. The Fecht and Gleiter method thus provides a means of locating the ORs that correspond to local minima in interfacial energy. The approach developed here also aims to identify energy cusps in OR space. However, rather than depositing randomly oriented particles on the substrate, copper crystals have been prepared by thin film deposition, followed by conversion of the thin film into particles, by two different approaches. In the first approach the copper film was dewetted in the solid state, whereas in the second approach the film was dewetted in the liquid state by raising the temperature above the melting point of copper and then freezing the resulting copper droplets.

Beyond growing copper particles by two different methods, particular attention has been paid to several details of the sample preparation procedure. Sapphire substrates were carefully prepared under well-defined conditions, and the impurities that segregated to the copper and sapphire surfaces were monitored by surface analytical techniques. This paper reports on new ORs that develop between copper and the c-plane of sapphire, gives estimates of the relative interfacial energies associated with the various ORs, and provides a discussion of their possible origins.

2. Experimental procedures

Copper films were deposited on sapphire (0 0 0 1) substrates and subsequently dewetted to form isolated copper crystals. The substrates consisted of single side epi-polished sapphire wafers, 5.08 cm in diameter, purchased from Gavish Industrial Technologies & Materials (Omer, Israel). These crystals have a maximum miscut of 0.1°, and the maximum impurity concentrations: 20 p.p.m. Mg, 15 p.p.m. Si, 10 p.p.m. Na, 7 p.p.m. Ca and 0.5 p.p.m. K. After ultrasonic cleaning in ethanol for a few minutes the surface chemistry of the wafers was investigated by Auger electron spectroscopy (AES), and found to consist of Al and O species with traces of C contamination.

The sapphire substrates were first annealed for several tens of hours at 1253 K under an Ar–20% O_2 atmosphere in a furnace fitted with a sapphire tube as described in Curiotto and Chatain [9]. After annealing and cooling to room temperature the sapphire surfaces were reanalyzed by AES to identify species which may have segregated to the surface, or were deposited from the environment, during annealing. The three cleanest substrates were selected for copper deposition, subsequently referred to as TC20, TC22 and TC25. Table 1 summarizes the main features of these samples. Ca was detected on all the samples, together with traces of Mo on TC22 and TC25. C contamination was acquired during sample transfer through air. Taking into account the size of the Auger peaks and the coverage calculated for Ca [9], the total coverage of metallic impurities is estimated to be about 0.3 monolayers. The surface morphologies were investigated by atomic force microscopy (AFM) using a Park model XE-100 instrument. They are shown in Fig. 1. Because surface impurities accelerate diffusion [9], TC22 and TC25 have fully formed steps, whereas on TC20 the steps have reached the same height (0.2 nm) but still display rough edges. The width of the terraces on all substrates is about 500 nm.

After substrate preparation the copper films were deposited by physical vapor deposition (PVD) in a UHV chamber fitted with capabilities for AES analysis. Copper was evaporated from a tungsten basket heated above the melting point of copper. The basket was located in a cylinder at a distance of 5 cm from the sample, with the copper flux exiting through a 8 mm orifice almost in contact with the substrate. After deposition the film surface was analyzed by AES, and traces of S and Cl were detected. These species were removed during subsequent annealing of the film under Ar–H_2 [10]. The film thickness ranged from 50 to 100 nm, as measured by AFM.

The last stage of preparation is formation of the copper crystals by dewetting of the copper films under an Ar–20% H_2 atmosphere. For this step the sapphire–copper samples were once again transferred to the sapphire furnace. During experimental runs the oxygen partial pressure, $p(O_2)$, of the flowing gas was controlled downstream from the sample at about 10^{-21} atm by means of an external electrochemical oxygen sensor, as described in Chatain et al. [11]. After a stable $p(O_2)$ was established the copper films were dewetted either in the solid state at 1253 K (TC25) or in the liquid state (TC20 and TC22). The diameter of the resulting copper particles was about 1 μm or less. Samples dewetted in the solid state were heated to a temperature of 1253 K for 78 h. For dewetting in the liquid state the temperature was set slightly above the copper melting point (1357 K) for 5 min. The samples were cooled to 1000 K over a period of 40 min to overcome possible undercooling of the liquid and solidify the droplets. Then the temperature was reset to the annealing temperature of 1253 K for several hours for equilibration of the copper–sapphire interface without excessive evaporation of the copper particles.

A dual beam focused ion beam (FIB) (Strata 400, FEI) was used to prepare transmission electron microscopy (TEM) specimens from the center of particles with a known morphology and orientation using the in situ "lift-out" technique [12]. The particles were sectioned through the Wulff point, in a direction carefully chosen to intersect specific surface facets for subsequent edge on imaging of the facets by TEM. Prior to sectioning a protective layer (of Pt or C) was deposited in order to prevent surface damage by the ion beam.

The morphology of the particles was examined by TEM using a monochromated and aberration corrected field emission gun-transmission electron microscope (FEI Titan 80-300 S/TEM) operated at 300 kV. Kikuchi electron diffraction was used to align the copper particles in a low index zone axis, with surface facets parallel to the viewing direction.

A detailed study on the atomistic structure of the interface is not the focus of this paper and the discussion will use

Table 1
Characteristics of the samples.

	TC20	TC22	TC25
Annealing time at 1253 K of sapphire substrates under Ar–O_2	78 h	78 h	122 h
Sapphire substrate surface impurities (AES)	C, Ca	C, Ca, Mo	C, Ca, Mo
Sapphire substrate step edge shape	Rough	Smooth	Smooth
Dewetting of the Cu film	Liquid	Liquid	Solid
Annealing time at 1253 K of Cu film under Ar–H_2 after dewetting	20 h	6 h	78 h

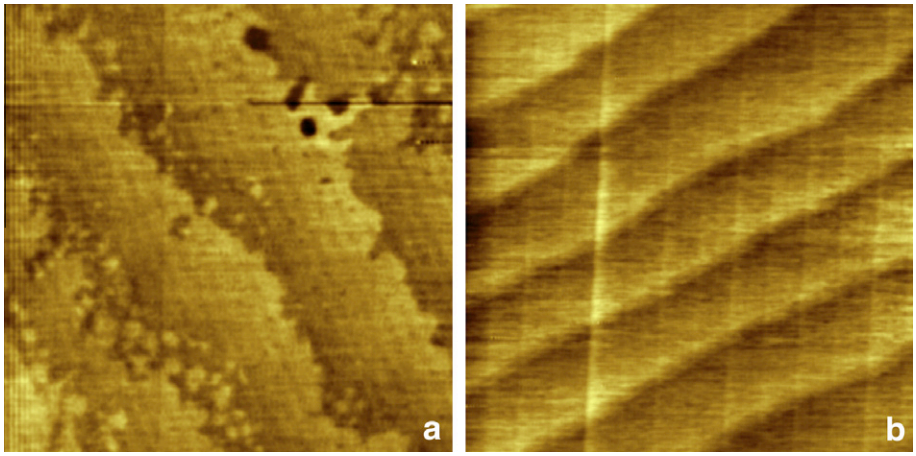

Fig. 1. 2×2 μm AFM micrographs of the surface morphology of the c-sapphire substrates. Brighter contrast is correlated with higher regions on the sample. In both cases there are terraces and steps with edges running along the $\langle 2\bar{1}\bar{1}0 \rangle$ direction. (a) TC20, the step edges are rough; (b) TC22 (and TC25), the step edges are smooth.

existing observations (see Section 4). High resolution TEM investigations of the Cu–Al_2O_3 interfaces are in progress. However, we emphasize that under the conditions of oxygen partial pressure and temperature in which the samples were prepared none of the mixed oxides ($CuAlO_2$ or $CuAlO_4$) can form at the interface. Indeed, at the temperature of our experiments these aluminates are stable only at an oxygen partial pressure higher than 7.2×10^{-8} atm [13].

3. Results and analysis

3.1. Copper crystal shape

Fig. 2a and b presents scanning electron microscopy (SEM) (JEOL, JMS-6320F) plan view micrographs of the copper particles. These images were obtained after carbon coating the samples to avoid charging effects. The copper particles are either single crystals or polycrystalline. When formed by dewetting in the liquid state their shape is more equiaxed, and their size distribution is more homogeneous. In both cases the crystals are almost fully faceted, with {1 1 1} and {1 0 0} facets. They do not have the equilibrium crystal shape (ECS) of copper at 1253 K, which is known from previous studies to be close to a sphere truncated by small {1 1 1} and {1 0 0} facets (maximum surface energy anisotropy of 2%) [10]. However, that previous study also showed that crystallites smaller than about 6 μm in diameter were likely to be more faceted than the ECS, due to inhibited nucleation kinetics for the growth or shrinkage of facets [14]. The more significant faceting of the present small crystallites is therefore not surprising.

The relatively large facet size is very useful for determination of the crystallographic directions of the copper crystals that are normal to the sapphire substrate, as this also identifies the copper interface plane. With the help of Wulffman freeware [15] these directions can be estimated from the symmetries of the facets. The most frequent copper orientations observed by SEM are given in Fig. 2c–f. These correspond to copper (1 1 1), (1 1 0), (3 1 1) and (2 1 0) interface plane orientations. In addition, it is useful to mention that about 70% of the particles in the liquid state dewetted samples (TC20 and TC22) are polycrystalline, with the majority being bicrystals containing a twin boundary. This trend was previously observed for gold particles on sapphire [16].

The faceted crystal shape also enables the selection of crystals to be sliced by FIB to produce TEM samples. These samples were used for observation of the copper–sapphire interfaces, for the determination of orientation relationships (ORs) by electron diffraction, and for the measurement of relative copper–sapphire interfacial energies.

3.2. EBSD analysis of copper particles on sapphire

An OR between two crystals is generally defined by specifying the interface planes in each of the two crystals and an in-plane direction of one crystal that is parallel to an in-plane direction of the other. The ORs between the

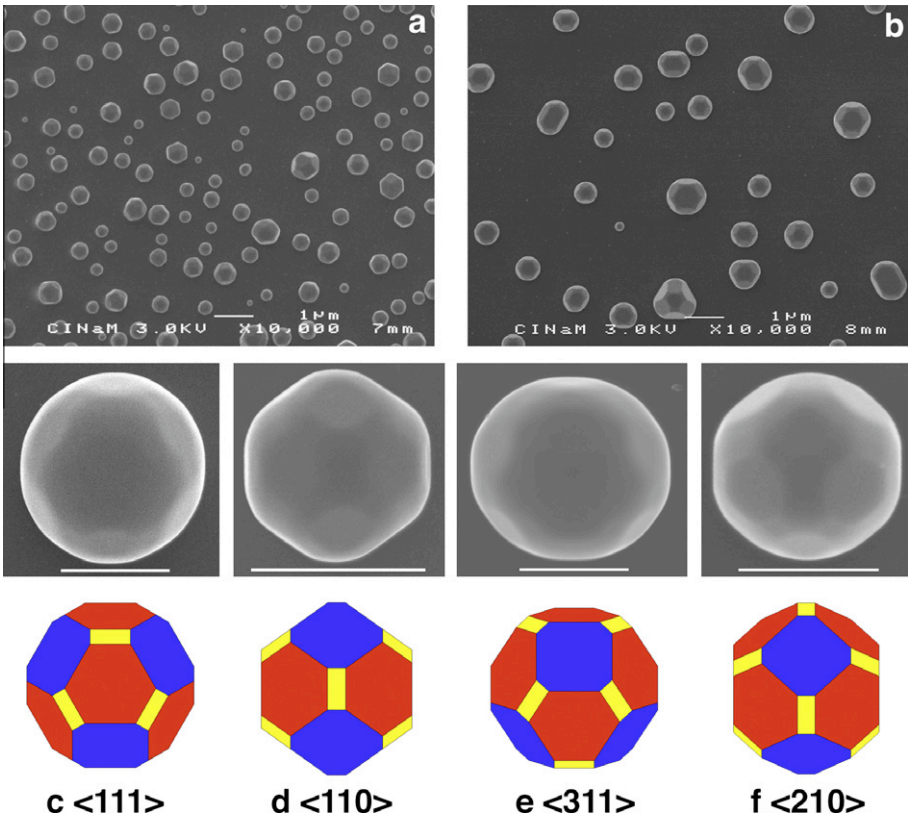

Fig. 2. Secondary electron SEM micrographs of: (a) copper crystals after liquid state dewetting; (b) copper crystals after solid state dewetting; (c)–(f) observed crystal shapes (from either (a) or (b)) with scale bars of 1 μm, and fcc crystal shapes calculated with Wulffman software (http://www.ctcms.nist.gov/archives/software/wulffman) viewed along the ⟨1 1 1⟩, ⟨1 1 0⟩, ⟨3 1 1⟩, and ⟨2 1 0⟩ directions, respectively. The {1 1 1}, {1 0 0}, and {1 1 0} facets are colored red, blue and yellow, respectively. (For interpretation of the references to color in this figure legend, the reader is referred to the web version of this article.)

copper crystals and the (0 0 0 1)-oriented sapphire substrate were determined by automated electron backscatter diffraction (EBSD) mapping in a FEI Quanta 200 FE ESEM equipped with an EDAX/TSL orientation system and the Hikara high speed EBSD detector. Data were collected at 30 kV with a 70° tilt of the sample. EBSD was previously used to follow the influence of annealing time on the ORs of gold particles on sapphire [16,17]. Since the SEM observations of the samples dewetted in the liquid state showed that the copper–sapphire OR is not unique (see Fig. 2a), we have developed a methodology to acquire sets of orientation data that extend over several hundred particles. For each sample the sapphire orientation was first quickly recorded (using 1 min data acquisition, so as to limit charge accumulation on the sapphire substrate) from a small area without copper particles. Then up to 10 carbon-coated areas with copper particles were scanned in steps of 50 nm and the EBSD patterns were recorded and simultaneously analyzed against the copper reference. In order to limit drift due to substrate charging each scan had to be acquired within 1 h. Finally, the EBSD maps from all acquisitions on the copper particles were merged for the purpose of determining the relative frequencies of appearance of the various ORs.

Fig. 3 shows a secondary electron SEM image of a typical area with copper particles onto which the EBSD copper map acquired from this region has been superimposed. The EBSD data were analyzed with the TSL-OIM software. The background of incorrectly identified points was removed from the orientation map by thresholding the confidence index at a value above one-third of the average value. Only the crystallographic orientation of the top of the particles is properly identified because of their curvatures and the collection angle of the EBSD detector [18]. With a scanning step of 50 nm it was possible to obtain orientation data of particles as small as 200 nm. The orientation data were analyzed in three different ways: (1) all the points measured on all the particles were considered (in this case large particles contribute more to the orientation data); (2) only one point per particle (or grain, when the particles are polycrystalline) was considered, so as to eliminate the influence of particle size; (3) particles with grain boundaries (GBs) were considered one at a time, so as to identify the misorientation between the grains.

ORs were determined using pole figures (PFs) and/or inverse pole figures (IPFs) obtained from the EBSD data, as discussed in Sections 3.4 and 3.5. These data allow identification of the copper planes parallel to the sapphire

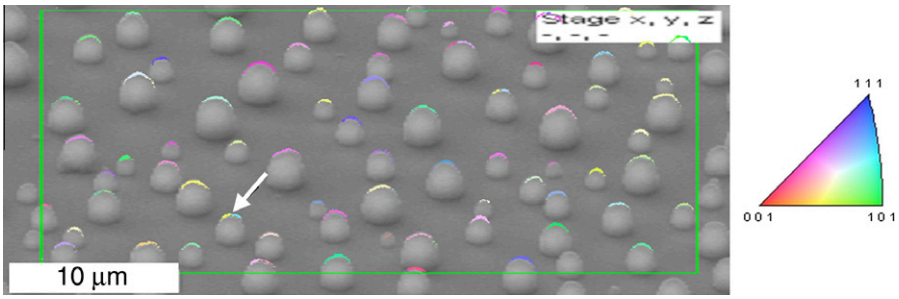

Fig. 3. Secondary electron SEM micrograph of copper particles and, superimposed in color, the EBSD copper map of the identified part of the crystals. The color code, on the right, corresponds to the IPF of copper in the [0 0 1] direction of the microscope reference frame, which is close to the normal of the sapphire surface. Particles containing grain boundaries (GBs) can be identified by the presence of more than one orientation (color) associated with a specific particle (see arrow). (For interpretation of the references to color in this figure legend, the reader is referred to the web version of this article.)

substrate and the in-plane directions of copper that lie parallel to densely packed directions of the c-plane of sapphire.

3.3. Polycrystalline particles

We have seen from the SEM study of samples dewetted in the liquid state that the most frequent, or preferred, interface planes displayed by copper particles are the (1 1 1), (1 1 0), (3 1 1) and (2 1 0) planes (Fig. 2). Confirmation of these trends by EBSD will be discussed below in Sections 3.4 and 3.5. However, since many of the particles contain GBs it is useful to mention that the majority of the GBs in polycrystalline particles are misoriented by 60°, indicating that they are most likely to be twin boundaries. These GB misorientations were determined from EBSD information, such as that shown in Fig. 3. This EBSD-based approach does not identify all GBs, as they may not intercept the small region of the particle for which orientation data is acquired. Table 2 summarizes all the possible normal directions of copper crystals due to the presence of twins for each of the four high frequency copper interface planes found in liquid dewetted samples (cf. Fig. 2c–f).

3.4. OR of crystals obtained by solid state dewetting

SEM micrographs (such as Fig. 2b) show that copper crystals formed by solid state dewetting are all oriented such that Cu(1 1 1)||Al_2O_3(0 0 0 1). From the location of the three {1 1 1} side facets (the brightest ones in Fig. 2b) we identify two equivalent orientation relationships rotated by 60° about the [1 1 1] direction of copper. This is consistent with either the double positioning due to stacking of Cu (1 1 1) atomic planes or with the 3-fold symmetry of the Al_2O_3(0 0 0 1) plane.

Table 2
Normal directions of twinned crystals.

Primary Cu interface plane	Other possible normal directions in twin-related crystals		
Cu(1 1 1)	⟨1 1 1⟩	⟨5 1 1⟩	
Cu(1 1 0)	⟨1 1 0⟩	⟨4 1 1⟩	
Cu(3 1 1)	⟨3 1 1⟩	⟨7 5 5⟩	⟨7 7 1⟩
Cu(2 1 0)	⟨2 1 0⟩	⟨5 4 2⟩	

Analysis of the EBSD data also allows identification of the second part of the OR, namely determination of parallel directions in the copper and c-sapphire planes at the interface. Fig. 4 presents the results corresponding to a region of the sapphire substrate containing more than 100 copper crystals. Fig. 4a displays the sapphire PFs of three relevant directions. The central spot in PF(0 0 0 1) is not exactly centered, because the [0 0 0 1] direction of sapphire is tilted by about 3° from the normal of the microscope reference frame (due to the small error in alignment of the sample in the sample holder). By chance, the two densest in-plane directions of Al_2O_3(0 0 0 1), namely [1 0 $\bar{1}$ 0] and [2 $\bar{1}$ $\bar{1}$ 0], fall almost parallel to the [0 1 0] and [1 0 0] directions of the microscope reference frame, respectively. Fig. 4b displays the cumulative (1 1 1), (1 1 0) and (2 1 1) PFs of copper particles. We see that the spots on the circular edge of PF(110) of copper occur at the same locations as the spots of PF (1 0 $\bar{1}$ 0) of sapphire (see the arrows in Fig. 4). This shows that the OR of the copper crystals on the sapphire is Cu(1 1 1) [1 $\bar{1}$ 0] ||Al_2O_3(0 0 0 1) [1 0 $\bar{1}$ 0] (OR1). Cu crystals with this OR can have two different orientation variants and therefore produce two different sets of spots in the PFs (red and black in Fig. 4b). The information given by the two right-most PFs is crystallographically redundant because Al_2O_3 [1 0 $\bar{1}$ 0] and Cu [1 $\bar{1}$ 0] are perpendicular to Al_2O_3 [2 $\bar{1}$ $\bar{1}$ 0] and Cu [1 1 $\bar{2}$], respectively. The minimum error of the EBSD analysis between two crystals (sapphire and copper) is ±0.5°. The data for the copper crystals are somewhat scattered due to their spherical shape: the EBSD patterns measured from point to point on a given crystal deviate by ±2°. Thus the experimental error on the OR determined by EBSD is about ±2.5°.

3.5. OR of crystals obtained by liquid state dewetting

In the two samples where the copper film was dewetted in the liquid state, TC20 and TC22, SEM observations showed that the particles are not uniquely oriented (Fig. 2a), and that many of them are polycrystalline. In order to identify

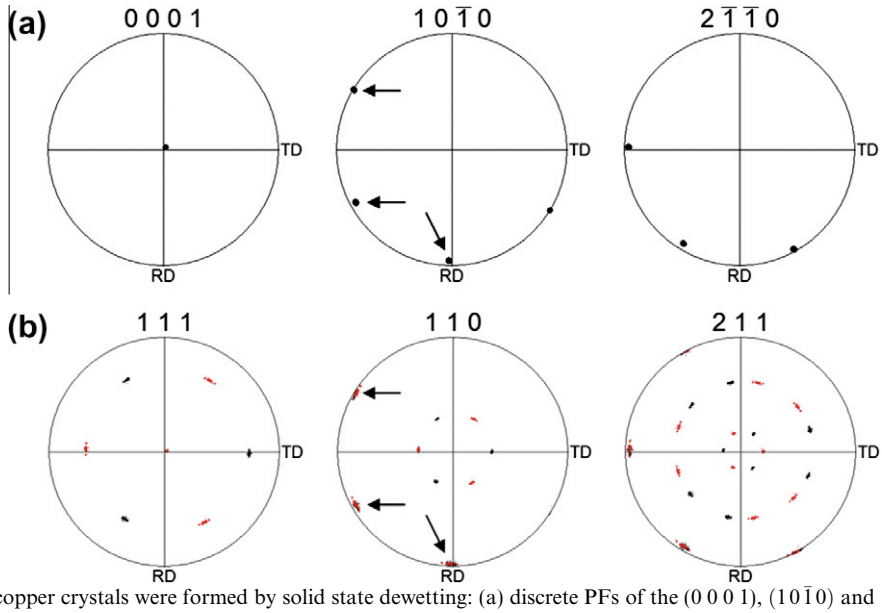

Fig. 4. PFs of TC25, where copper crystals were formed by solid state dewetting: (a) discrete PFs of the (0 0 0 1), (1 0 $\bar{1}$ 0) and (2 $\bar{1}$ $\bar{1}$ 0) planes of sapphire; (b) discrete cumulative PFs of the {1 1 1}, {1 1 0} and {2 1 1} planes of 103 copper particles (see text).

the most frequent ORs between the copper crystals and the sapphire (0 0 0 1) substrate an analysis of the orientations of more than 500 copper particles was performed for each sample. To avoid biasing of the results due to the largest crystals only one point per crystal was included in the analysis. Fig. 5 shows the IPF in the [0 0 1] direction of the microscope reference frame for the copper particles of TC20. This direction is tilted by ~3° from the [0 0 0 1] sapphire direction. There are four preferred copper planes parallel to the sapphire c-plane: (1 1 1), (3 1 1), (2 1 0) and (1 1 0). Actually, these planes are only 2–2.4 times more probable than the average, as indicated by the multiples of random distribution (MRD) bar shown in Fig. 5. For TC22 the results are qualitatively identical (i.e. the same copper planes are preferred, but in a somewhat different order of frequency). The four interfacial copper planes found by EBSD are the same as those identified by SEM using the Wulffman sketches in Fig. 2c–f.

The complete OR for each of the four preferred copper interface plane orientations identified in Fig. 5 was determined using the TSL-OIM software. Copper PFs were constructed from the data for each type of preferred plane selected on the IPF of Fig. 5 in order to identify the copper

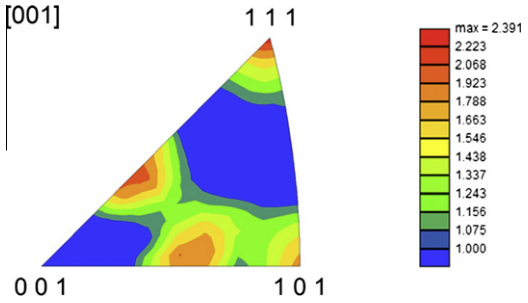

Fig. 5. IPF showing the frequency of copper planes parallel to the substrate in TC20, as quantified in units of MRD in the inset. The data have been obtained from 530 crystals, with only one datum per crystal.

directions parallel to the two most densely packed directions of sapphire: Al_2O_3 [1 0 $\bar{1}$ 0] and Al_2O_3 [2 $\bar{1}$ $\bar{1}$ 0]. The relevant PFs of sapphire and copper are shown in Fig. 6, and Table 3 summarizes the results.

Before discussing the results related to the in-plane crystallographic symmetries of the Al_2O_3(0 0 0 1) plane and of the copper interface planes some points need to be emphasized. The two densest directions of the Al_2O_3(0 0 0 1) plane (Al_2O_3 [1 0 $\bar{1}$ 0] and Al_2O_3 [2 $\bar{1}$ $\bar{1}$ 0]) lie at 90° to each other, and both have 3-fold in-plane symmetry about the [0 0 0 1] direction. Among the four copper planes of interest only the Cu(1 1 1) plane contains directions with a 3-fold symmetry. The three other preferred interface planes have only 2-fold symmetry, however, they can each be positioned on the sapphire substrate in three different variants that are equivalent. Table 3 identifies the two directions in the copper interface plane, Cu[u' v' w'] and Cu[u'' v'' w''], that are parallel to the two densest directions of sapphire. Although this crystallographic information is redundant, it is useful for a discussion of the results in the framework of existing models of ORs [7].

We now turn to Fig. 6. The top row of the figure gives selected PFs of the sapphire substrate together with a schematic of the surface structure of the c-sapphire surface. The next four rows of the figure display selected PFs as well as schematics of the surface structures of the four high frequency Cu interface planes.

For copper crystals with a (1 1 1) interfacial plane there are two ORs: either Cu [1 $\bar{1}$ 0]||Al_2O_3 [1 0 $\bar{1}$ 0] (OR1) or Cu [1 $\bar{1}$ 0]||Al_2O_3 [2 $\bar{1}$ $\bar{1}$ 0] (OR2). For each of these ORs there are two equivalent variants rotated by 180° about the [1 1 1] direction of copper. In PF(1 1 0) for the copper (1 1 1) interfacial plane each single crystal of OR1 produces three spots on the outer edge and three spots located 35° from the center of the PF. For crystals with OR1 both variants are displayed, leading to a doubling of the spots to six.

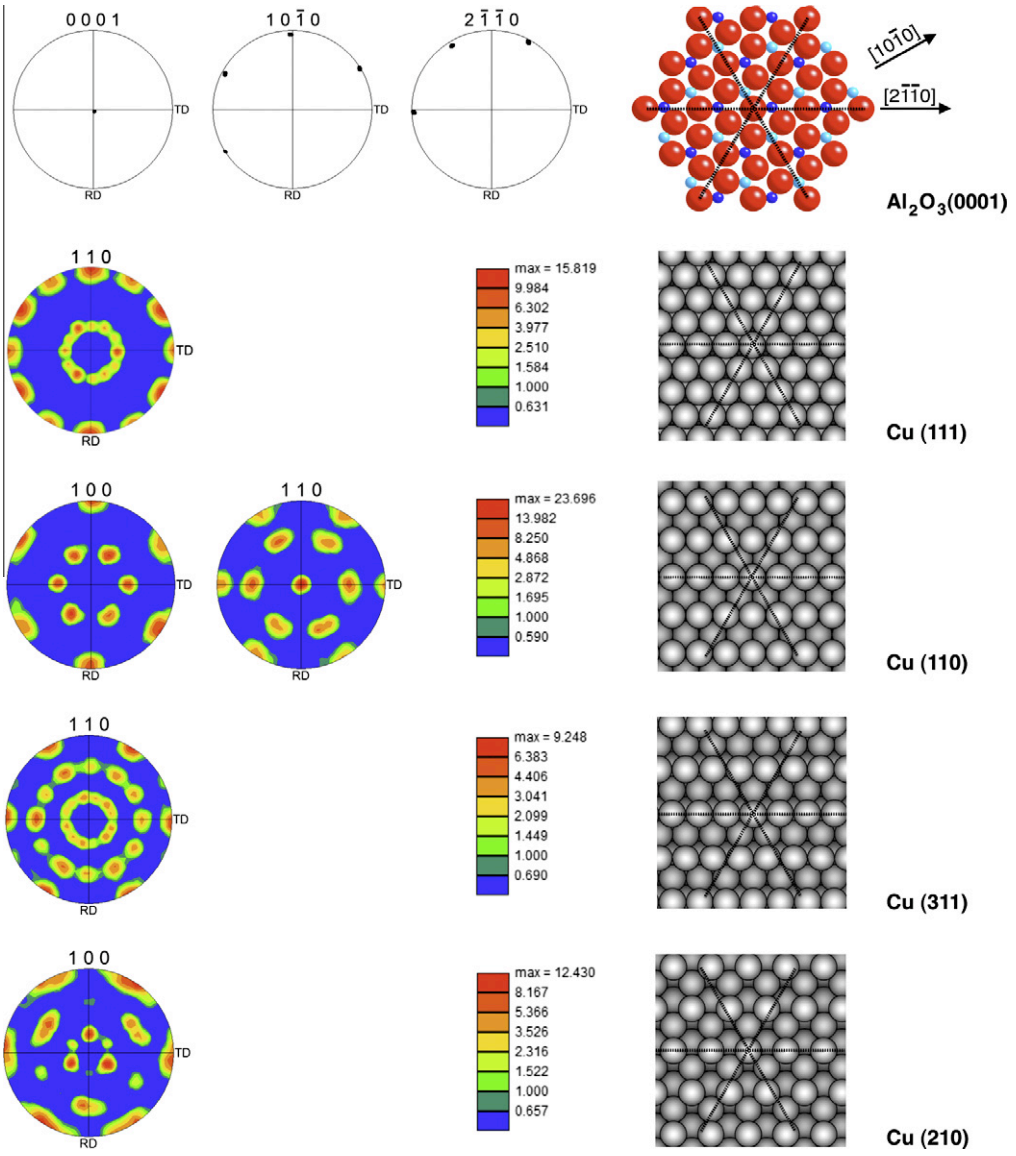

Fig. 6. Comparison of the PFs of sapphire and copper from sample TC22 in the relevant directions for the four interface planes identified in Fig. 5. (Upper panel) The PFs of the (0 0 0 1), (1 0 $\bar{1}$ 0) and (2 $\bar{1}$ $\bar{1}$ 0) planes of sapphire on the left, and the atomic arrangement at the unreconstructed sapphire surface on the right (one oxygen layer sandwiched between two aluminum layers, where large and small circles represent O^{2-} and Al^{3+} ions, respectively; two colors have been used for the two different Al ion planes). (Lower panel) The left side of the four panels give copper PFs of various orientations obtained from crystals displaying (1 1 1), (1 1 0), (3 1 1) and (2 1 0) interface planes, respectively. The location of the spots on the circular edge of the copper PFs should be compared with each of the sapphire PFs. If the spots are superimposed the corresponding copper and sapphire directions are parallel. A PF may contain several variants of an OR. The right-most boxes of the four panels show sketches of the four different copper interface planes on which are superimposed the traces of the three Al_2O_3 ⟨2 $\bar{1}$ $\bar{1}$ 0⟩ directions (see text).

Table 3
ORs of copper crystals dewetted in the liquid state on Al_2O_3(0001).

Cu{*h k l*}‖Al_2O_3(0 0 0 1)	Cu⟨*u′v′w′*⟩‖Al_2O_3 ⟨1 0 $\bar{1}$ 0⟩	Cu⟨*u″ v″ w″*⟩‖ Al_2O_3 ⟨2 $\bar{1}$ $\bar{1}$ 0⟩
{1 1 1}	⟨**1 1 0**⟩ OR1	⟨2 1 1⟩
{1 1 1}	⟨2 1 1⟩ OR2	⟨**1 1 0**⟩
{1 1 0}	⟨1 0 0⟩	⟨**1 1 0**⟩ OR3
{3 1 1}	⟨3 3 2⟩	⟨**1 1 0**⟩ OR4
{2 1 0}	⟨2 1 0⟩	⟨**0 0 1**⟩ OR5

Each line corresponds to a single OR, with the densest in-plane copper direction indicated in bold.

However, there are also some crystals that display OR2. The two variants of these crystals lead to another six spots on the outer edge and at 35° from the center of the PF. These additional spots occur at 30° to those belonging to

OR1. Although only OR1 is found by solid state dewetting (see Fig. 4), liquid state dewetting produces both OR1 and OR2. Based on the relative intensities of the spots from OR1 and OR2 (in MRD units) it seems that OR1 appears at a somewhat higher frequency than OR2.

For copper crystals with a (1 1 0) interface plane there is only one OR: Cu $[1\bar{1}0]\|Al_2O_3$ $[2\bar{1}\bar{1}0]$, which will be referred to as OR3. This OR could equivalently be described as Cu$[0\,0\,1]\|Al_2O_3$ $[10\bar{1}0]$). In the (1 1 0) interface plane of each copper crystal there is only one $\langle 1\,1\,0\rangle$ and one $\langle 1\,0\,0\rangle$ direction (see the sketch of the atomic structure of the (1 1 0) plane in Fig. 6). The six $\langle 1\,1\,0\rangle$ spots on the outer edge of PF(1 1 0) correspond to three different but equivalent variants of the OR. Similarly, the six $\langle 1\,0\,0\rangle$ spots on the edge of PF(1 0 0) are also due to the same three different possible variants. In addition, it is important to recognize that for a given variant, with a $\langle 1\,1\,0\rangle$ direction aligned with Al_2O_3 $[2\bar{1}\bar{1}0]$, there are necessarily two higher index $\langle u\,v\,w\rangle$ directions aligned with other members of the Al_2O_3 $\langle 2\bar{1}\bar{1}0\rangle$ family of directions. These high index directions would also appear with relatively high frequency in an IPF based on particles that have a (1 1 0) interface plane, but their presence is a direct consequence of the alignment of the $[1\bar{1}0]$ direction with Al_2O_3 $[2\bar{1}\bar{1}0]$. Thus if the ORs are determined from IPFs alone there is a danger of assigning undue importance to in-plane high index directions that appear for geometric reasons.

For the copper crystals with a (3 1 1) interface plane there is one OR: Cu $[1\bar{1}0]\|Al_2O_3$ $[2\bar{1}\bar{1}0]$. This OR will be referred to as OR4. Again, for any given copper crystal the only in-plane Cu $\langle 1\,1\,0\rangle$ direction is parallel to one of the three Al_2O_3 $\langle 2\bar{1}\bar{1}0\rangle$ directions. The corresponding in-plane copper row parallel to Al_2O_3 $\langle 10\bar{1}0\rangle$ is Cu $\langle 3\,3\,2\rangle$. As in the crystals with a Cu(1 1 0) interface plane, there are three equivalent variants of the OR. Additional faint spots on the outer circle of PF(1 1 0) for this orientation (Fig. 6) arise from grains with a Cu(3 1 1) plane parallel to the substrate that are in twin-related orientations to the grains with OR4 (see Table 2).

In the case of crystals with a Cu(2 1 0) interface plane it is clear from PF(1 0 0) shown in Fig. 6 that the $\langle 1\,0\,0\rangle$ in-plane directions of Cu are aligned with the Al_2O_3 $[2\bar{1}\bar{1}0]$ directions. This OR, Cu$[0\,0\,1]\|Al_2O_3$ $[2\bar{1}\bar{1}0]$, will be referred to as OR5. However, the spots in PF(1 0 0) are quite elongated compared with the PFs shown for other interfacial planes. This is because there are two possible Cu $\langle 2\,1\,0\rangle$ directions normal to the substrate that correspond to twin-related orientations (see Table 2), and elongation of the spots corresponds to near overlap (~10°) of the spots originating from the two twins.

3.6. TEM study of copper–sapphire interface shape and energy anisotropy

Confirmation of the ORs and measurement of the relative interface energies between copper and sapphire were performed by cross-section TEM of selected copper crystals prepared using a dual beam FIB, as previously described for gold particles supported on sapphire [16,19]. In the FIB copper crystals with (1 1 1), (1 1 0), (3 1 1) and (2 1 0) interface planes were prepared from samples dewetted in the liquid state (all from sample TC20). Fig. 7 shows a bright field TEM micrograph of a particle with a Cu(1 1 1) interface plane, sectioned through the middle, in a direction perpendicular to the sapphire substrate. Altogether six copper crystals were investigated, two with Cu(3 1 1), two with Cu(1 1 1) and one each with Cu(1 1 0) and Cu(2 1 0) interface planes.

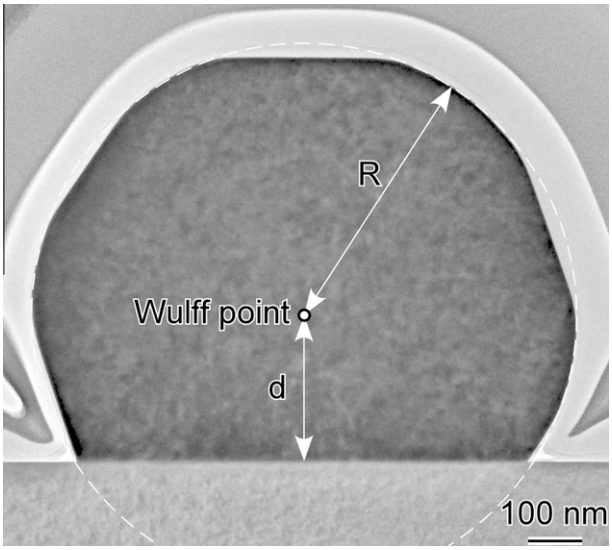

Fig. 7. Bright field TEM micrograph of a copper particle with a (1 1 1) interfacial orientation. The center of the circle through the curved particle surfaces corresponds to the Wulff point, which may then be used to define R and d, the respective distances to the round surfaces and the substrate.

ORs for these crystals were determined from selected area electron diffraction patterns after aligning the samples in a low index zone axes using Kikuchi electron diffraction, which is a more accurate (although statistically limited) approach than EBSD. These measurements confirmed the orientation relationships determined by EBSD, with the exception of OR1, for which a 2° tilt was observed between the Cu(1 1 1) interface plane and Al_2O_3(0 0 0 1). The TEM measurements also showed that the copper–sapphire interfaces were flat over their entire lengths at the nanometer length scale. Furthermore, from images such as Fig. 7 it is possible to use the Winterbottom construction [20] (see, for example, Sadan and Kaplan [16]) to estimate the relative copper–sapphire interfacial energy for the five observed ORs. This construction is also illustrated in Fig. 7, and can be expressed as follows:

$$\frac{R}{d} = \frac{\gamma_{mv}}{\gamma_{mo} - \gamma_{ov}} \quad (1)$$

where R and d are the distances from the Wulff point of the crystal (see Fig. 7) to a rounded surface region and to the substrate, respectively, γ_{mv}, γ_{ov} and γ_{mo}, are the energies of the metal–vapor interface corresponding to the rounded

(roughened) parts of the particle surface, the oxide–vapor interfacial energy and the metal–oxide interfacial energy, respectively.

Taking the surface energy of solid copper (1520 ± 75 mJ m^{-2} in the range 1223–1283 K [21]) and the surface energy of sapphire (0 0 0 1) (1280 ± 80 mJ m^{-2} at 1173 K, 1242 ± 80 mJ m^{-2} at 1253 K, with a temperature coefficient of 0.474 mJ m^{-2} K^{-1} [22]) the Cu($h\ k\ l$)/Al_2O_3(0 0 0 1) interfacial energies can be estimated from the Winterbottom construction. These are summarized in Table 4. The table also includes the "equivalent contact angle" θ for the particles, defined by $\cos\theta = -d/R$. The values of Table 4 are generally consistent with the interfacial energy between liquid copper and Al_2O_3(0 0 0 1), i.e. 2060 ± 150 mJ m^{-2}, obtained from the surface energy and the contact angle of liquid copper (1350 ± 50 mJ m^{-2} and $\theta = 130 \pm 2°$, respectively) given by Ghetta et al. [23].

4. Discussion

4.1. General considerations regarding ORs

There are several factors that can cause a specific OR to develop at an interface joining crystals of two different phases. Lattice mismatch between the two phases can lead to interfaces that are coherent, semi-coherent or incoherent. At coherent interfaces the lattice planes of both phases match across the interface plane, whereas no matching occurs in the case of incoherent interfaces. Semi-coherency results when different lattice spacings across the interface are adjusted by the presence of a periodic network of interfacial dislocations. However, the specific type of interface that develops in any particular system results from an optimization of the factors that control interfacial energy, including both elastic strain energy and contributions from chemical bonding interactions that occur across the interface.

In the case of copper–c-plane sapphire interfaces the lattice periodicities across the interface are quite different for all of the copper interface planes observed in this study. For example, in the ORs observed for the case of Cu(1 1 1) interfacial planes, such as OR1 and OR2, the existence of coherent interfaces would lead to elastic strains of the order of $\pm 7\%$, presumably on the softer copper side of the interface. Such large strains, and the resulting high strain energies, rule out interface coherency and one therefore expects those interfaces to be either incoherent or semi-coherent. There is experimental evidence available to support the existence of both incoherent [5,24] and semi-coherent interfaces [6] at those ORs.

4.2. Substrate chemistry and ORs

In the past the chemical termination of c-plane sapphire substrates has been considered to play a significant role in the resulting OR. However, the present results, taken in conjunction with previous studies, tend to indicate that the chemical nature of the sapphire surface does not play a dominant role in the resulting OR.

The c-sapphire surface can be terminated in various ways: by a single Al layer (stoichiometric or Al1-terminated), two aluminum layers (aluminum-rich or Al2-terminated), or O-terminated (O-rich termination) [25]. It is also possible to prepare an OH-terminated c-sapphire surface, although this termination does not survive exposure to temperatures above ~873 K [26]. Under the conditions of our experiments, in which sample equilibration was performed under an oxygen partial pressure of about 10^{-21} atm at 1253 K, the copper–sapphire system thermodynamics indicate that the sapphire surface should be Al1-terminated [27,28].

The OR1 and OR2 ORs, identified here for Cu(1 1 1) interface planes, have also been observed in previous studies. For example, Oh et al. [6] found that OR1 develops in continuous copper films grown on the OH-terminated c-plane of sapphire, whereas OR2 develops when (1 1 1) textured copper films grown on O-terminated c-sapphire are annealed at 773 K. Dehm et al. reported that the development of both OR1 and OR2 in copper films at 373–473 K is very sensitive to growth temperature and deposition rate [29] and speculated that these two ORs may have a similar interfacial energy (which we have now proved to be correct at 1253 K, see Table 4). It is worth noting that OR2 was also found in the case of gold particles on c-sapphire produced by liquid state dewetting of a gold film under an atmosphere containing oxygen, i.e. under conditions that should produce an O-terminated sapphire surface [16]. In the present study we have observed OR2 on an Al1-terminated c-sapphire surfaces, as well as a number of previously unreported ORs in liquid state dewetted samples. Thus, there does not appear to be a unique substrate termination that is associated with the appearance of OR2.

Table 4
Energy anisotropy of Cu($h\ k\ l$)/Al_2O_3(0 0 0 1) interfaces.

OR and Cu interface plane	R/d	Equivalent contact angle (°)	Estimated interfacial energy (mJ m^{-2})
OR1 Cu(1 1 1)	2.05	119	1982 ± 120
OR2 Cu(1 1 1)	1.86	123	2060 ± 120
OR3 Cu(1 1 0)	2.06	119	1979 ± 120
OR4 Cu(3 1 1)a	2.04	119	1987 ± 120
OR4 Cu(3 1 1)b	1.83	123	2073 ± 120
OR5 Cu(2 1 0)	1.96	121	2016 ± 120

First principles calculations were used to investigate the atomistic structures and the energetics of OR1 and OR2 [30]. This paper reports approximately similar calculated works of separation for OR1 and OR2 (6.5 and 6.9 J m^{-2}) when sapphire is oxygen terminated, which leads the authors to conclude that the two ORs have comparable interfacial energies. While this conclusion is consistent with our measurements reported in Table 4, the calculated values of the work of separation are one order of magnitude higher than those we have found experimentally (using the surface energy of copper and the measured equivalent contact angle in Table 4 we get a work of separation of 0.8 J m^{-2}). In the same paper Hashibon et al. calculated a work of separation of 0.7 J m^{-2} for OR1 with an Al-terminated sapphire interface, which is in agreement with our measurements. This suggests that the sapphire interfaces are not O-terminated at the oxygen partial pressures of our experiments.

One last point about the surface composition of the substrate may be worth mentioning. The substrates for samples dewetted in the liquid state, TC20 and TC22, had different surface contaminations (see Table 1), but the ORs obtained on these two substrates were essentially identical. Thus it is unlikely that the contaminants detected by AES on the sapphire surface prior to copper deposition play a major role in the observed ORs.

4.3. Comparison with the Fecht and Gleiter lock-in model

Fecht and Gleiter [7] have reported the most comprehensive study of ORs observed for isolated gold and copper crystallites supported on ionic substrates. Their aim was to allow crystallites to freely "rotate" into the OR most closely corresponding to a cusp in the dependence of interfacial energy on orientation, as had been shown previously in the seminal paper on copper grain boundaries by Herrmann et al. [8]. They investigated a number of ionic substrate orientations, specifically the (1 1 1), (1 1 0) and (1 0 0) planes of several cubic ionic crystals and the (0 0 0 1) plane of sapphire. Their conclusions regarding the ORs that occur with frequencies above random can be summarized as follows: (1) coincidence site lattice ORs are not observed; (2) the observed ORs are those where the metal interfacial planes are low index and where the most densely packed direction in the interface plane of the fcc metal (i.e. ⟨1 1 0⟩) is aligned with a relatively densely packed direction of the substrate. Since they found that the alignment of relatively densely packed directions was present in all the observed high frequency ORs they concluded that it is an essential feature of these ORs. They rationalized these observations by postulating that low energy interfaces could form if the atoms on the metallic side of the interface tended to fit into the valleys present along densely packed directions of the ionic surface, and termed the phenomenon the lock-in mechanism. The frequency with which they observed the lock-in mechanism was greater for cases with smaller lattice mismatches.

It is worth noting that Fecht and Gleiter [7], who identified high frequency ORs from PFs obtained by X-ray diffraction, did not detect any preferred OR for copper crystals (0.5–2 μm in size) on the c-plane of sapphire after annealing at 823 K for 5 h. The crystals they investigated were initially prepared like ours, but then detached and redeposited on a fresh c-plane of sapphire before equilibration [7,31]. Many of their particles may therefore have been polycrystalline from the first preparation step, thereby reducing the observed fraction of oriented crystals.

The observations reported here are in general agreement with the lock-in postulate of Fecht and Gleiter. In the case of solid state dewetting only OR1 is observed, in which Cu [1 $\bar{1}$ 0] is aligned with Al_2O_3 [1 0 $\bar{1}$ 0], whereas in liquid state dewetting five ORs are observed, four of which have ⟨1 1 0⟩ close packed directions of copper aligned with one of the two densely packed directions of c-sapphire. The only exception is OR5, with a Cu(2 1 0) interface plane, that does not contain the ⟨1 1 0⟩ direction. However, even in this case we find a parallel alignment of Cu[0 0 1] with Al_2O_3 [2 $\bar{1}$ $\bar{1}$ 0], i.e. two relatively densely packed directions.

Although the ORs that were observed to occur at relatively high frequency in this study are consistent with the lock-in model, it is not clear why the alignment of relatively densely packed directions should be so prevalent in the ORs of metal phases supported on ionic substrates. After all, the rationale for the lock-in mechanism, i.e. the fitting of metal atoms into the valleys associated with densely packed rows of the substrate structure, lacks a convincing physical basis. It may be that an experimental study of the microscopic degrees of freedom at these interfaces, i.e. the local atomistic structure, will shed light on the reason for the alignment of densely packed directions. Experiments on this issue are currently being conducted.

4.4. Differences between solid and liquid state dewetting

There are some substantial differences between the ORs observed after solid and liquid state dewetting. In the solid state dewetted sample only OR1 is observed, whereas the samples dewetted in the liquid state display five higher than random ORs, including OR1 and OR2 for crystals with a Cu(1 1 1) interface plane, as well as crystals with OR3, OR4 and OR5, all of which have their most densely packed directions parallel to the c-sapphire [2 $\bar{1}$ $\bar{1}$ 0] direction. The following interpretations are proposed to explain these results.

We first address the results obtained by liquid state dewetting. In this case the resulting copper particles are formed by solidification of liquid droplets, a process that involves nucleation of the solid phase somewhere within the liquid drop. Nucleation could occur homogeneously in the bulk of the liquid drop. Under those conditions one would expect the initial solidified droplets to have random ORs with respect to the substrate. During the subsequent equilibration treatment the solid crystallites could rotate in order to lower their energy by adopting ORs that

correspond to cusp orientations in terms of the dependence of interfacial energy on orientation. However, formation of a solid nucleus by heterogeneous nucleation on the substrate is expected to be kinetically preferred over formation by homogeneous nucleation in the body of the liquid, far from the interface. Thus we favor an interpretation that relies on heterogeneous nucleation during solidification. This implies that favored nuclei would occur for ORs where the solid Cu–sapphire interfacial energy is relatively low, since the two other interfaces of a nucleus, namely the solid copper–liquid copper, and the liquid copper–sapphire interfaces, have approximately equal energies for all the observed ORs. Based on the present estimates of relative interfacial energies (Table 4) all the interfaces found in the higher frequency ORs have approximately equal interfacial energies (within the estimated errors) and therefore appear with above random frequencies that are all rather similar.

Models were constructed of the five interfacial structures that result from superimposition of each of the four preferred copper interface planes on the c-sapphire plane for the five observed ORs. The lattice constants on both sides of these interfaces were chosen to correspond either to their room temperature or 1253 K values. No particularly significant crystallographic or chemical coincidences were found. Thus no particular reason for the observed ORs could be identified.

It is interesting to recall that the surfaces of the c-sapphire substrates used in this study consist of steps lying along a single $[2\bar{1}\bar{1}0]$ direction (Fig. 1). Although these steps could conceivably play a role in the nucleation of solid copper from the liquid, this does not appear to be the case. Evidence for this can be found in the PFs for the (1 1 0), (3 1 1) and (2 1 0) copper planes shown in Fig. 6, where it can be seen that the three OR variants appear with equal frequency. If nucleation on the pre-existing $[2\bar{1}\bar{1}0]$ steps was favored the two other OR variants would tend to be suppressed.

It should also be noted that the c-sapphire surface undergoes several reconstructions at temperatures above 1273 K. According to the observations of Gauthier et al. [32] it is possible to infer that the (1×1) c-sapphire surface undergoes reconstruction to a $(2\sqrt{3} \times 2\sqrt{3})R30°$ structure somewhere between 1273 and 1373 K. The latter structure undergoes a further transition to a $(3\sqrt{3} \times 3\sqrt{3})R30°$ structure between 1373 and 1523 K, and, finally, a $(\sqrt{31} \times \sqrt{31})R \pm 9°$ structure appears somewhere between 1523 and 1623 K. Thus it is possible for the first of these high temperature structures to form during liquid state dewetting at temperatures close to the melting temperature of copper (1356 K). Although the atomistic structure of the $(2\sqrt{3} \times 2\sqrt{3})R30°$ reconstruction equilibrated in contact with copper is not known [33], its presence could conceivably lead to the formation of a dense direction at 30° to Al_2O_3 $[10\bar{1}0]$. This might explain the apparent alignment of the dense copper directions on Al_2O_3 $[2\bar{1}\bar{1}0]$ for ORs 2–5. Although the structures present at the free c-sapphire surface need not be the same as those that are stable at copper–c-sapphire interfaces, recent observations of the structure of the nickel–c-sapphire interface after solid state dewetting and equilibration at 1623 K have shown the presence of a structure similar to the $(3\sqrt{3} \times 3\sqrt{3})R30°$ [34]. Some evidence therefore exists to support the persistence of c-sapphire surface reconstructions at metal–c-sapphire interfaces that are similar to the copper–c-sapphire interface.

We now turn to the OR observed in the case of solid state dewetting. The "as deposited" copper films, prior to dewetting, display a strong (1 1 1) texture, i.e. the grains of the film are predominantly oriented with their (1 1 1) planes parallel to the sapphire substrate. Solid state dewetting occurs during heating of the films to the equilibration temperature of 1253 K. After equilibration of the films for 78 h virtually all copper crystals display OR1. There are two possible scenarios that can lead to the development of the very high frequency of crystallites with OR1. One possibility is that grains in the film which happen to be oriented according to OR1 consume other grains during grain growth preceding dewetting. The other possibility is that dewetting occurs first and that crystallites oriented according to OR1 consume other particles by an Ostwald ripening-like process. Either of these scenarios implies that crystallites oriented according to OR1 have the lowest energy of crystallites which display a Cu(1 1 1) interface plane.

During the preparation of copper particles by solid state dewetting the temperature does not exceed 1253 K. Since reconstructions of the c-sapphire surface that lead to a 30° rotation of the surface Bravais unit cell occur above 1273 K this may explain the absence of OR2 in samples dewetted in the solid state.

Whereas the interpretations suggested above to explain the differences between the ORs observed as a result of solid state versus liquid state dewetting seem plausible, one observation in the liquid state dewetted samples is still difficult to account for, the fact that both OR1 and OR2 are observed in those samples. If ORs 2–5 arise because reconstruction of the copper–c-sapphire interface leads to a 30° rotation of the structural unit cell on the c-sapphire side of the interface, why then is OR1 still present in liquid state dewetted samples? No persuasive answer to this question has been found.

5. Conclusions

Depending on the method adopted to dewet copper from the surface of c-sapphire substrates, it is possible to obtain quite different ORs. Solid state dewetting produces a single OR: Cu(1 1 1) $[1\bar{1}0]$ ‖sapphire(0 0 0 1) $[10\bar{1}0]$ (OR1). In contrast, liquid state dewetting produces four new ORs with (1 1 1), (1 1 0), (3 1 1) and (2 1 0) copper interface planes, in which the most densely packed direction on the copper side of the interface is aligned parallel to the sapphire $[2\bar{1}\bar{1}0]$ direction. The ORs that include (1 1 0), (3 1 1) and (2 1 0) copper interface planes have not been previously observed.

One possible explanation of the change in the alignment direction on the c-sapphire side of the interface for liquid state dewetted samples is a reconstruction of the copper–c-sapphire interface, similar to the c-sapphire surface reconstruction that is known to occur at temperatures above 1273 K, i.e. above the highest exposure temperature of solid state dewetting but below the highest temperature to which the liquid state dewetted samples were exposed.

Although Cu(1 1 1) [1 $\bar{1}$ 0]||sapphire(0 0 0 1) [2 $\bar{1}$ $\bar{1}$ 0] (OR2) has been observed before, its appearance has been linked to a change in substrate chemistry from that at which OR1 develops. The present results show that OR2 can occur for a range of substrate chemistries, including the same chemistry as the one which also favors the development of OR1.

All of the observed ORs are consistent with the Fecht and Gleiter lock-in mechanism, which argues for the development of ORs that have low index interface planes in which relatively densely packed directions on both sides of the interface are aligned.

Acknowledgements

The authors thank A.D. Rollett for useful discussions and S. Labat for XRD analyses. H.M. and W.D.K. acknowledge support from the Russell Berrie Institute for Nanotechnology at the Technion. D.C., H.M. and W.D.K. acknowledge partial support from the Ministry of Science and Technology, Israel, and the Ministry of Research, France. This document has been produced with the partial financial assistance of the European Union as part of the MACAN project as part of the Seventh Framework Programme (2007–2013) under grant agreement FP7-NMP-2009-CSA-233484. Lastly, H.C., P.W. and G.S.R. acknowledge support of their research by the MRSEC Program of the National Science Foundation under award no. DMR-0520425.

References

[1] Katz G. Appl Phys Lett 1968;12:161.
[2] Moller PJ, Guo Q. Thin Solid Films 1991;201:267.
[3] Susnitzky DW, Barry Carter C. Surf Sci 1992;265:127.
[4] Bialas H, Knoll E. Vacuum 1994;45:959.
[5] Scheu C, Gao M, Oh SH, Dehm G, Klein S, Tomsia AP, et al. J Mater Sci 2006;41:5161.
[6] Oh SH, Scheu C, Wagner T, Ruhle M. Appl Phys Lett 2007;91:141912.
[7] Fecht HJ, Gleiter H. Acta Metall 1985;33:557.
[8] Herrmann G, Gleiter H, Bäro G. Acta Metall 1976;24:353.
[9] Curiotto S, Chatain D. Surf Sci 2009;603:2688.
[10] Chatain D, Ghetta V, Wynblatt P. Interf Sci 2004;12:7.
[11] Chatain D, Chabert F, Ghetta V, Fouletier J. J Am Ceram Soc 1993;76:1568.
[12] Reyntjens S, Puers R. J Micromech Microeng 2001;11:287.
[13] Trumble KP. Acta Metall Mater 1992;40:s105.
[14] Mullins WW, Rohrer GS. J Am Ceram Soc 2000;83:214.
[15] Roosen AR, McCormack RP, Carter WC. Comput Mater Sci 1998;11:16.
[16] Sadan H, Kaplan WD. J Mater Sci 2006;41:5099.
[17] Sadan H, Kaplan WD. J Mater Sci 2006;41:5371.
[18] Chatain D, Galy D. J Mater Sci 2006;41:7769.
[19] Baram M, Kaplan WD. J Microsc 2008;232:395.
[20] Winterbottom WL. Acta Metall 1967;15:303.
[21] Kumikov VM, Khokonov KB. J Appl Phys 1983;54:1346.
[22] Levi G, Kaplan WD. Acta Mater 2003;51:2793.
[23] Ghetta V, Fouletier J, Chatain D. Acta Mater 1996;44:1927.
[24] Dehm G, Rühle M, Ding G, Raj R. Philos Mag B 1995;71:1111.
[25] Batyrev I, Alavi A, Finnis M. Faraday Discuss 1999;114:33.
[26] Fu Q, Wagner T, Ruhle M. Surf Sci 2006;600:4870.
[27] Saiz E, Cannon RM, Tomsia AP. Acta Mater 1999;47:4209.
[28] Zhang W, Smith JR, Evans AG. Acta Mater 2002;50:3803.
[29] Dehm G, Edongue H, Wagner T, Oh SH, Arzt E. Z Metallkd 2005;96:249.
[30] Hashibon A, Elsässer C, Rühle M. Acta Mater 2005;53:5323.
[31] Erb U, Abel W, Gleiter H. Scripta Metall 1982;16:1317.
[32] Gautier M, Renaud G, Pham Van L, Villette B, Pollak M, Thromat N, et al. J Am Ceram Soc 1994;77:323.
[33] Vilfan I, Deutsch T, Lancon F, Renaud G. Surf Sci 2002;505:L215.
[34] Meltzman H, in press.